วารสารวิชาการเทคโนโลยีอุตสาหกรรม (The Journal of Industrial Technology)
ISSN (Print): 1686-9869, ISSN (online): 2697-5548
DOI: 10.14416/j.ind.tech.2022.12.001

บทความวิจัย

Influences of Aging and Inflation Pressure on Stiffness and Absorbed Energy of a Passenger Car Radial Tire

Supasit Nantapuk, Sathaporn Chuepeng and Manida Tongroon*

ATAE Research Unit, Department of Mechanical Engineering, Faculty of Engineering at Sriracha, Kasetsart University

* Corresponding author, E-mail: manida@eng.src.ku.ac.th

Received: 6 October 2022; Revised: 12 July 2022; Accepted: 26 July 2022
Online Published: 14 December 2022

Abstract: The objective of this study is to investigate the influences of aging and inflation pressure on the stiffness and absorbed energy of radial tires. By quasi-static compression test, new and 50,000-km used tires were determined for acting force and corresponding displacement. Between the 172.4 kPa and 241.3 kPa inflation pressure range for the new tire, the load was linearly increased with displacement. The absorbed energy was non-linear increasing with the displacement. The trend of the accumulative absorbed energy was increased when inflated the tire pressure. For both new and used tires, the stiffness and the absorbed energy were linearly increasing with the inflation pressure. The used tire was harder than the new tire observed by the higher tire stiffness and can be absorbed greater energy. At the rated inflation pressure of 220.6 kPa, after 50,000 km usage, the tire was intensified by 2.62% in terms of stiffness and by 2.22% in terms of energy absorbed. On average, over the inflation pressure in the range of 172.4 kPa to 241.3 kPa, the stiffness and absorbed energy were by 3.22 % and 2.98 % increase for the aging tire compared to the base new tire.

Keywords: car; energy; passenger; stiffness; suspension; tire

วารสารวิชาการเทคโนโลยีอุตสาหกรรม (The Journal of Industrial Technology)
ISSN (Print): 1686-9869, ISSN (online): 2697-5548
DOI: 10.14416/j.ind.tech.2022.12.001

1. Introduction

The tire is a friction material that plays a vital role in vehicle stability and performance. A driving power source requires tires to transmit a traction force onto road pavement through transmission and driveline systems [1]. Tires are the first contact between a car's chassis and road surface [2], especially during cornering under lateral force. Tires are in a suspension system of a vehicle that has to bear vehicle weight and road-generated vibration [3]. New-developed tires are, therefore, concerned with all performance aspects.

In an aspect of the suspension part, the tire has been modeled in various manners [4]. In a mass-spring-damper vibration model, the tire is usually considered as a spring and/or damper [5] with a complex nonlinear system [6]. Yu et al. (2016) [7] simulated a combined stiffness of leaf spring and tire assembly. Kim et al. (2015) [8] equipped a sensor to the tire and measured the strain that occurred. The hardware in the loop (HIL) system was simulated to study behavior. The measured strain has been founded to link with force and energy related to lose in terms of acoustic [9], especially tire texture that can generate different noise spectra [10].

During traction, longitudinal friction force performs its duty in sprint driving the vehicle [11]. In particular when cornering where a tire may deform [12], tire-road friction coefficient and tire stiffness change depending on vehicle weight and speed [13]. This generates rolling resistance [14-15] and the roughness of the road excites the contact surface of the tire generating a vertical force perpendicular to the traction. These lateral, vertical, and longitudinal forces are combined as an input to the vehicle's mass-spring-damper system that has to be properly managed [16].

Parts of these force-derived energies can be harvested [17]. Roshani et al. (2016) [18] collected asphalt pavement road vehicle-induced stresses and transfer them into electricity through the piezoelectric disks. Later on, energy harvesting systems from dampers (shock absorbers) have been developed by Zhang et al. (2017) [19] and Zhang et al. (2018) [20]. For the tire itself, Maurya et al. (2018) [21] made an energy harvesting and strain sensing system for the autonomous vehicle. The system provides a power output of approx. 580 μW at 16 Hz from the energy harvester mounted on a section of a tire that can power 78 LEDs. From these scenarios, tire stiffness plays an important role in the effects of other resultant outcomes and is also affected by other parameters concerned.

Stiffness in every part of the tire and directions that forces act on can be determined by various methods [22]. Misiewicz et al. (2016) [23] estimated the carcass stiffness of agricultural tires on hard surfaces. The tire load-deflection method was used under a variation of inflation pressure 0.5 to 2.5×10^5

วารสารวิชาการเทคโนโลยีอุตสาหกรรม (The Journal of Industrial Technology)
ISSN (Print): 1686-9869, ISSN (online): 2697-5548
DOI: 10.14416/j.ind.tech.2022.12.001

Pa. The load was founded to increase with increasing deflection. Liu and Gao (2018) [24] analytically investigated nonlinear sidewall stiffness. The rigid-elastic coupled tire model was employed with heavy truck tires under impulsive loading conditions. Liu et al. (2019) [25] modeled the combined sidewall stiffness of heavy-loaded off-road tires. The sidewall radial stiffness was directly increased with increasing inflation pressure in the range of 0.3 to 0.8 MPa. Xu et al. (2022) [26] studied the structural performance of tyre walls on a full scale. A hydraulic loaded puncher with LVDT was equipped in the test machine to in determining the force and lateral displacement of the tires in a lump scale. The lateral stiffness declined during increasing lateral displacement.

While a car is in movement, tire stiffness is altered to some certain extent. Xu and Ahmadian (2013) [27] improved stiffness and damping suspension systems on tire load transfer during cornering. A nonlinear variable stiffness tire model was simulated whereas normal (vertical) and braking (longitudinal) forces were determined depending on time and conditional excitation applied. In the meantime, Soltani et al. (2015) [28] optimized tire vertical stiffness based on the ride, handling, performance, and fuel consumption criteria. The optimized tire stiffness was in the range of 100 to 300 N/mm up on certain criteria chosen. Lian et al. (2015) [29] estimated cornering stiffness and sideslip angle by simplifying lateral dynamic models for an electric vehicle using lateral tire force data. After simplification, the front and rear cornering stiffness were reduced, to the maximum values of 80 and 30 kN/rad, respectively. Ni et al. (2017) [30] expanded tyre cornering stiffness simulation for AWD electric vehicles to analyze for static stability. Lateral and longitudinal forces were dependent on vertical load and slip ratios. During rotation, Kim (2009) [31] numerically simulated the rotational stiffness of radial tires. The rotational stiffness of the tire was directly increasing with leveling inflation pressure in the range of 50 to 300 kPa. Its behavior was explained by the macroscopic shear modulus of carcass ply and sidewall.

In aspects of the material, different constituents of tire parts cause a diverse stiffness behavior. Tao et al. (2018) [32] integrated carbon nanotubes and rubber composites as the cord. By simple swelling and infusion method, these smart cords were viable to sense interfacial strain and damage from static and cyclic loadings. By static electro-mechanical test, its stiffness was constant; the loads were linearly proportioned to the displacement in the range of 15 to 25 mm. Low-hysteresis run-flat tire was investigated by Bae et al. (2019) [33] for structural and vertical stiffnesses by considering strain energy. Vertical stiffness with linear relation to the inflation pressure of the run-flat tire was higher than that of the regular tire. Li et al. (2020) [34]

วารสารวิชาการเทคโนโลยีอุตสาหกรรม (The Journal of Industrial Technology)
ISSN (Print): 1686-9869, ISSN (online): 2697-5548
DOI: 10.14416/j.ind.tech.2022.12.001

doped the Al_2O_3 - rGO network to enhance the mechanical strength of natural rubber nanocomposites. In addition, compounded tread rubber-affected winter tires were also investigated by Shenvi et al. (2022) [35].

Other independent parameters can affect tire stiffness dependent on the conditions applied. Pillai (2006) [36] Inflation pressure effect on whole tire hysteresis ratio and radial stiffness. Linear correlations between stiffness and inflation pressure were proposed. Tire-road contact stiffness was simulated by Winroth et al. (2014) [37]. The contact stiffness was nonlinear to the indentation while the contact force was linearly increasing with the indentation after 0.05 mm. Wright et al. (2019) [38] worked on SUV tire aging that was worn in certain conditions; these changed the tire stiffness and friction properties. For agricultural tires, stiffness changed as a function of tire wear was reported by Becker and Els (2022) [39].

Previously published works have used vehicle tire types as specimens of their studies, even for a variety of materials used as tire's parts. Meanwhile, limited work has been done on the stiffness change that results in the absorbed energy of radial tire. Besides, there is less available information for aging tire and inflation pressure impacted on these independent parameters. In subsequentness, some other aspects have not yet been revealed according to these matters.

The objective of this study is to investigate the influences of aging and inflation pressure on stiffness and absorbed energy of the radial tires. By quasi-static compression test, a new and 50,000-km used tires were determined for acting force and corresponding displacement. In this scheme, load and absorbed energy behavior were first explored. Dependency of tire stiffness and absorbed energy on inflation pressure will be later disclosed. Lastly, the influences of tire aging will be analyzed and discussed.

2. Materials and Method

2.1 Tire Characteristics and Composition

The experimental study was conducted using two tires with both 185/60 R15 sizes from the same manufacturer. One was a new tire and the other was a used tire (50,000 km, approx. 3 years). Both tires were newly manufactured in mid-2018 with a depth of 4.8±0.06 mm averaged from eight points along both longitudinal grooves at 220.6 kPa, 35°C. The tread pattern of the test tire and nomenclature are shown in Fig. 1. There were two wide longitudinal grooves symmetrically lined in the middle of the tire. Sipe and block in the middle isle were asymmetrically inclined.

The tire cross-section and compound are shown in Fig. 2. There are four key parts: liner, bead wires, sidewall, and tread which were made of composite materials. The sidewall and the tread

วารสารวิชาการเทคโนโลยีอุตสาหกรรม (The Journal of Industrial Technology)
ISSN (Print): 1686-9869, ISSN (online): 2697-5548
DOI: 10.14416/j.ind.tech.2022.12.001

were two-plied and made from polyester. The liner was a one-ply polyamide for material with two steel belts across the tire circle.

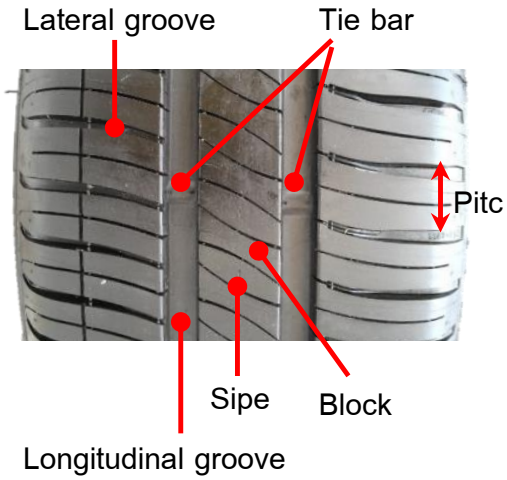

Fig. 1 Tread pattern of the test tire and nomenclature

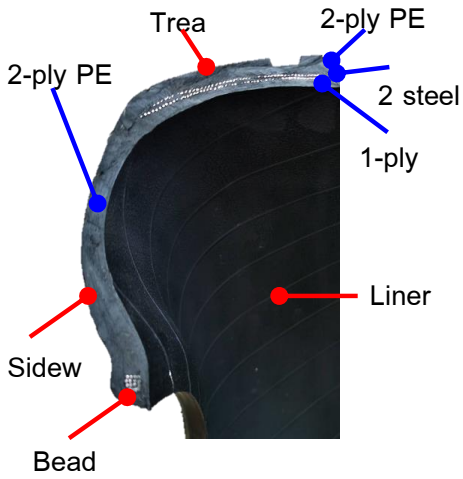

Fig. 2 Tire cross section and compound

2.2 Test Apparatus

The tires were tested by the quasi-static method using a Shimadzu Hydraulic Universal Testing Machine (Model: UH-1000kNX). The machine is a computer-controlled electro-hydraulic servo type. The force was measured by cylinder internal pressure with a high-precision pressure cell within ±1.0 % of the indicated value (when the force is 1/1 to 1/250 of the rated value). This conforms to JIS B7721 Class 1, ISO 7500/1 Class 1, and ASTM E4 standards. Its digital force was displayed with a resolution of 1/200,000. Its stroke measurement was by the optical encoder with a digital display in 0.01 mm resolution. The quasi-static test apparatus is depicted in Fig. 3.

Fig. 3 Quasi-static test apparatus

วารสารวิชาการเทคโนโลยีอุตสาหกรรม (The Journal of Industrial Technology)
ISSN (Print): 1686-9869, ISSN (online): 2697-5548
DOI: 10.14416/j.ind.tech.2022.12.001

2.3 Tire Stiffness and Absorbed Energy Determination

The Universal Testing Machine was capable of applying force as a load to the tire correspondingly under the measurement of displacement (stroke). The slope of the corresponding force and displacement is considered the global tire stiffness. Meanwhile, the area under the force-displacement curve is the absorbed energy. By this definition, accumulative absorbed energy over displacement can be readily calculated and properly displayed throughout the paper.

2.4 Test Condition and Method

Both tires were separately placed on the test machine under specified conditions. For the load and absorbed energy behavior study, each tire was inflated for the pressure value range of 172.4 kPa (25 psi) to 241.3 kPa (35 psi) with a gradual stepping increment of 7 kPa (1 psi). This inflation pressure range was chosen according to ±30% of recommended pressure value defined by the manufacturer. The stroke of the machine's puncher was set to 20 mm to mimic a real-life usage of the tire. All tests were repeated three times and each average value is representative of the analysis of each condition.

3. Results and Discussion

3.1 Load and Absorbed Energy Behavior

Fig. 4 shows the characterization of load dependency on displacement within a 20-mm stroke for the new tire. The quasi-static test was in the range of inflation pressure values between 172.4 kPa and 241.3 kPa. The load was linearly dependent on displacement for all inflation pressure values. At the maximum 20-mm stroke tested, the loads were ranging from 1.57 kN to 2.03 kN in accordance with 172.4 kPa to 241.3 kPa inflation pressure values, respectively. The increasing stroke resulted in the incremental force applied. This yields positive slopes of the load-stroke characteristics (stiffness) of the new tire. However, the trend of the slope seemingly escalated during the strengthening inflation pressure. The slope value (stiffness) will be shown and discussed later in the next section.

Fig. 5 shows the accumulative absorbed energy in correspondent with displacement within 20-mm stroke for the new tire. The accumulative absorbed energy is the consequence of the force load applied to the tire by the calculation scheme described in Section 2.3. The absorbed energy was non-linear to the displacement for all inflation pressure values. The increasing number of strokes has been seen to result in exponentially increasing energy

วารสารวิชาการเทคโนโลยีอุตสาหกรรม (The Journal of Industrial Technology)
ISSN (Print): 1686-9869, ISSN (online): 2697-5548
DOI: 10.14416/j.ind.tech.2022.12.001

that can be absorbed. The trend of the accumulative absorbed energy was increased when inflated the tire pressure. At the maximum 20-mm stroke tested, the maximum accumulative absorbed energy was 18.9 J at the maximum inflation pressure of 241.3 kPa.

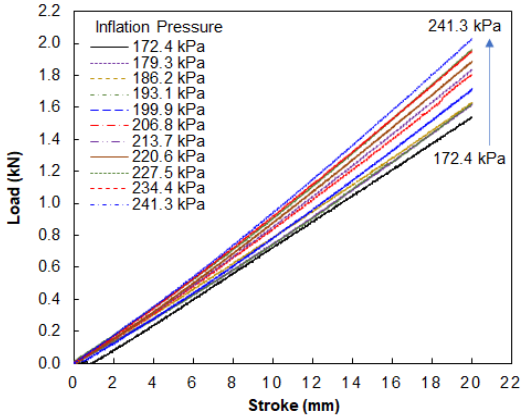

Fig. 4 Load-displacement (stroke) characteristics of the new tire

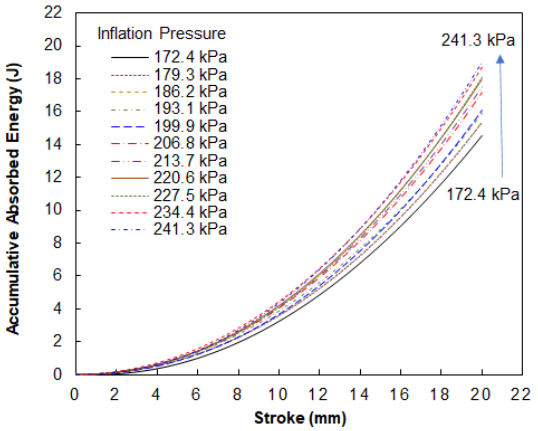

Fig. 5 Accumulative absorbed energy-displacement (stroke) characteristics of the new tire

3.2 Dependency of tire stiffness and absorbed energy on inflation pressure

After the load-stroke dependency was determined and described in the previous section, the tire stiffness can be plotted and shown in Fig. 6. The tire stiffness as calculated from the load-stroke characteristics is founded to be a linear function of the inflation pressure in the range of 172.4 kPa to 241.3 kPa. This behavior can be also observed for both new and used tires. In this range of inflation pressure, the stiffness values lie between 79.1 N/mm and 101.9 N/mm for the new tire. In the same inflation pressure range, the stiffness values were 80.3 N/mm to 102.9 N/mm for the used tire. The used tire was harder than the new tire as it displayed a higher tire stiffness. The linear regression of the tire stiffness and inflation pressure relationship was founded and can be proposed by Formula (1) and (2).

New tire:

$$\text{Stiffness (N/mm)} = 0.35 \times \text{Pressure (kPa)} + 17.292 \quad (1)$$

Used tire:

$$\text{Stiffness (N/mm)} = 0.3485 \times \text{Pressure (kPa)} + 20.457 \quad (2)$$

Fig. 7 shows the plots of accumulative absorbed energy and inflation pressure for both new and used tires. The absorbed energy as calculated from the load-stroke characteristics is also founded to be a linear function of the inflation pressure in the range of 172.4 kPa to 241.3 kPa.

วารสารวิชาการเทคโนโลยีอุตสาหกรรม (The Journal of Industrial Technology)
ISSN (Print): 1686-9869, ISSN (online): 2697-5548
DOI: 10.14416/j.ind.tech.2022.12.001

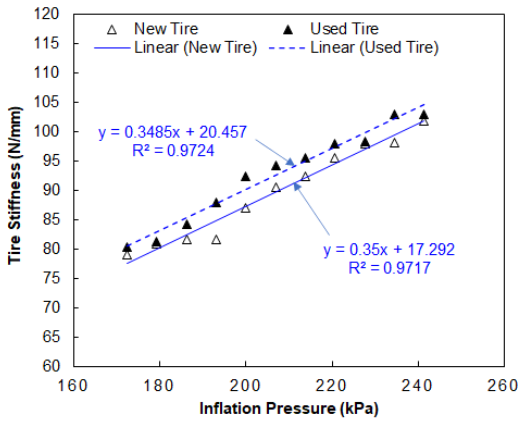

Fig. 6 Tire stiffness dependency on inflation pressure

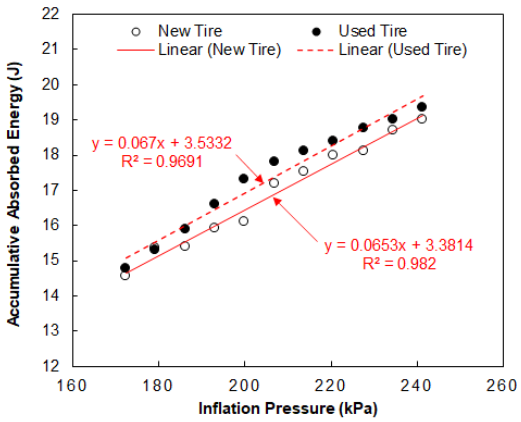

Fig. 7 Accumulative absorbed energy dependency on inflation pressure

This behavior can be also observed for both new and used tires. In this range of inflation pressure, the accumulative absorbed energies are between 14.5 J and 19.0 J for the new tire. In the same inflation pressure range, the accumulative absorbed energies were 14.8 J to 19.3 J for the used tire. The used tire which was harder can be absorbed greater energy than the new tire. The linear regression of the accumulative absorbed energy and inflation pressure relationship were founded and can be proposed by Formula (3) and (4).

New tire:

$$\text{Energy (J)} = 0.0653 \times \text{pressure (kPa)} + 3.3814 \quad (3)$$

Used tire:

$$\text{Energy (J)} = 0.0670 \times \text{pressure (kPa)} + 3.5332 \quad (4)$$

Fig. 9 explicitly shows the tire aging effects for stiffness at the rated inflation pressure of 220.6 kPa. During 50,000 km usage, the tire stiffness was intensified from 95.5 N/mm to 98.0 N/mm. This can be accounted for 2.62% in terms of stiffness. At the same rated inflation pressure of 220.6 kPa, during 50,000 km usage, the absorbed energy was strengthened from 18.0 J to 18.4 J (see Fig. 9 on the right axis). This can be accounted for 2.22% in terms of energy absorbed.

Fig. 10 shows the statistical incrementation in stiffness and absorbed energy of the used tire over the new tire. In detail, there was no trend observed for the incrementation of stiffness and absorbed energy against the inflation pressure values tested. The minimum and maximum incremental values of the used tire's stiffness and absorbed energy were 0 and 7.82%. On average, over the inflation

วารสารวิชาการเทคโนโลยีอุตสาหกรรม (The Journal of Industrial Technology)
ISSN (Print): 1686-9869, ISSN (online): 2697-5548
DOI: 10.14416/j.ind.tech.2022.12.001

pressure in the range of 172.4 kPa to 241.3 kPa, the stiffness and absorbed energy were by 3.22 % and 2.98 % increase for the aging tire (50,000 km) compared to the base new tire.

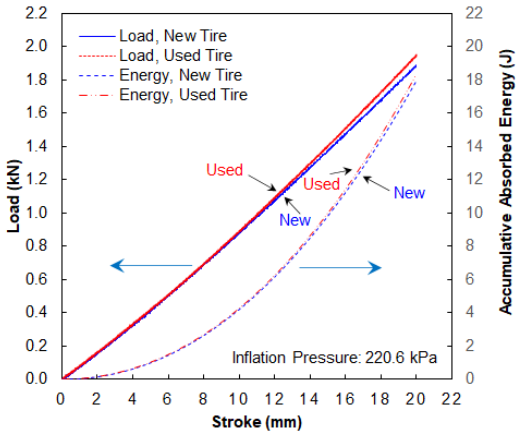

Fig. 8 Tire aging effects for load and absorbed energy characteristics, at 220.6 kPa inflation pressure

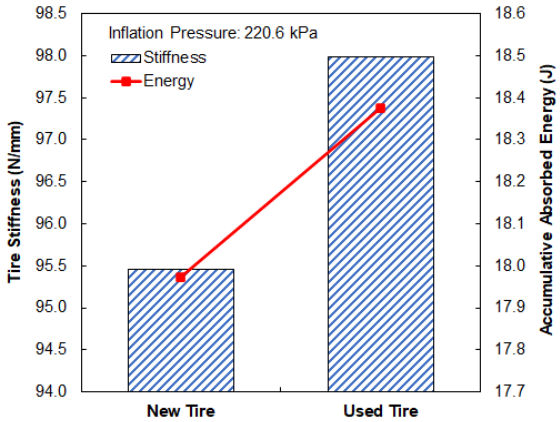

Fig. 9 Tire aging effects for stiffness and absorbed energy, at 220.6 kPa inflation pressure

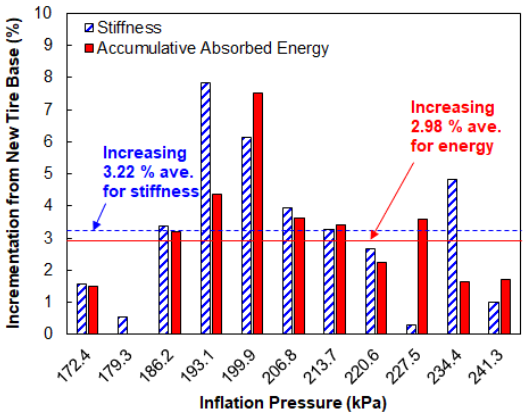

Fig. 10 Incrementation of stiffness and absorbed energy of the used and new tires

4. Conclusions

This work investigates the aging and inflation pressure effects on the stiffness and absorbed energy of radial tires. By quasi-static compression test, new and 50,000-km used tires were acted by force with corresponding displacement measurement. The conclusions can be drawn as the followings.

Between the 172.4 kPa and 241.3 kPa inflation pressure range for the new tire, the load was linearly increased with displacement up to the maximum 20-mm stroke tested. The stiffness seemingly escalated during the strengthening inflation pressure. The absorbed energy was non-linear increasing with the displacement. The trend of the accumulative absorbed energy was increased when inflated the tire pressure.

For both new and used tires, the stiffness from the load-stroke characteristics are founded to be a

วารสารวิชาการเทคโนโลยีอุตสาหกรรม (The Journal of Industrial Technology)
ISSN (Print): 1686-9869, ISSN (online): 2697-5548
DOI: 10.14416/j.ind.tech.2022.12.001

linear function of the inflation pressure in the range of 172.4 kPa to 241.3 kPa. The used tire was harder than the new tire as it displayed a higher tire stiffness. The stiffness values were maximized by 101.9 N/mm and 102.9 N/mm for the new and used tires, respectively. For both new and used tires, the absorbed energy is also founded to be a linear function of the inflation pressure in the range of 172.4 kPa to 241.3 kPa. The used tire which was harder can be absorbed greater energy than the new tire. The accumulative absorbed energies were maximized by 19.0 J and 19.3 J for the new and aging tires, respectively.

The results show a higher capacity to absorb the energy for the used tire over the new tire. At the rated inflation pressure of 220.6 kPa, during 50,000 km usage, the tire was intensified by 2.62% in terms of stiffness and by 2.22% in terms of energy absorbed. On average, over the inflation pressure in the range of 172.4 kPa to 241.3 kPa, the stiffness and absorbed energy were by 3.22 % and 2.98 % increase for the used tire compared to the base new tire.

The attained results could be a guideline for tire manufacturers in terms of rubber composition and structure suitable for pressure inflation, stiffness, and aging when in use. In the aspect of car users, care should be taken when using aging tires due to changes in tire properties under certain operating conditions.

5. Acknowledgement

Kasetsart University, Faculty of Engineering at Sriracha is acknowledged for financial support to this project (Project No. 2011/64).

6. References

[1] C. Becker and S. Els, Motion resistance measurements on large lug tyres, Journal of Terramechanics, 2020, 88, 17-27.

[2] E.S. Rødland, O.C. Lind, M. Reid, L.S. Heier, E. Skogsberg, B. Snilsberg, D. Gryteselv and S. Meland, Characterization of tire and road wear microplastic particle contamination in a road tunnel: From surface to release, Journal of Hazardous Materials, 2022, 435, 129032.

[3] T.V. Glazkov and S.A. Reshmin, A nonlinear tire model to describe an unwanted flat vibrations of the wheels, IFAC-PapersOnLine, 2019, 52(16), 268-273.

[4] Z. Liu and Q. Gao, Development of a flexible belt on an elastic multi-stiffness foundation tire model for a heavy load radial tire with a large section ratio, Mechanical Systems and Signal Processing, 2019, 123, 43-67.

[5] F. Braghin, F. Cheli and E. Sabbioni, Identification of tire model parameters through full vehicle experimental tests, Journal of Dynamic Systems, Measurement, and Control, 2011, 133(3), 031006.

วารสารวิชาการเทคโนโลยีอุตสาหกรรม (The Journal of Industrial Technology)
ISSN (Print): 1686-9869, ISSN (online): 2697-5548
DOI: 10.14416/j.ind.tech.2022.12.001

[6] H.-R.B. Bosch, H.A. Hamersma and P.S. Els, Parameterisation, validation and implementation of an all-terrain SUV FTire tyre model, Journal of Terramechanics, 2016, 67, 11-23.

[7] Z. Yu, Y. Liu, B. Tinsley and A.A. Shabana, Integration of geometry and analysis for vehicle system applications: Continuum-based leaf spring and tire assembly, Journal of Computational and Nonlinear Dynamics, 2016, 11(3), 031011.

[8] S.J. Kim, K.-S. Kim and Y.-S. Yoon, Development of a tire model based on an analysis of tire strain obtained by an intelligent tire system, International Journal of Automotive Technology, 2015, 16(5), 865-875.

[9] X. Hu, X. Liu, X. Wan, Y. Shan and J. Yi, Experimental analysis of sound field in the tire cavity arising from the acoustic cavity resonance, Applied Acoustics, 2020, 161, 107172.

[10] A. Del Pizzo, L. Teti, A. Moro, F. Bianco, L. Fredianelli and G. Licitra, Influence of texture on tyre road noise spectra in rubberized pavements, Applied Acoustics, 2020, 159, 107080.

[11] J. Hu, S, Rakheja and Y. Zhang, Tire-road friction coefficient estimation under constant vehicle speed control, IFAC- PapersOnLine, 2019, 52(8), 136-141.

[12] W. Zhao, C. Zhang and J. Zhang, Continuous measurement of tire deformation using long-gauge strain sensors, Mechanical Systems and Signal Processing, 2020, 142, 106782.

[13] R. Wang and J. Wang, Tire-road friction coefficient and tire cornering stiffness estimation based on longitudinal tire force difference generation, Control Engineering Practice, 2013, 21(1), 65-75.

[14] F. Li, F. Liu, J. Liu, Y. Gao, Y. Lu, J. Chen, H. Yang and L. Zhang, Thermo-mechanical coupling analysis of transient temperature and rolling resistance for solid rubber tire: Numerical simulation and experimental verification, Composites Science and Technology, 2018, 167, 404-410.

[15] Y. Gong, L. Zhao, J. Zhang and N. Hu, A novel model for determining the fatigue delamination resistance in composite laminates from a viewpoint of energy, Composites Science and Technology, 2018, 167, 489-496.

วารสารวิชาการเทคโนโลยีอุตสาหกรรม (The Journal of Industrial Technology)
ISSN (Print): 1686-9869, ISSN (online): 2697-5548
DOI: 10.14416/j.ind.tech.2022.12.001

[16] J. Lieh, Tire damping effect on ride quality of vehicles with active control suspensions, Journal of Vibration and Acoustics, 2009, 131(3), 031011.

[17] M.A.A. Abdelkareem, L. Xu, M.K.A. Ali, A. Elagouz, J. Mi, S. Guo, Y. Liu and L. Zuo, Vibration energy harvesting in automotive suspension system: A detailed Review, Applied Energy, 2018, 229, 672-699.

[18] H. Roshani, S. Dessouky, A. Montoya and A.T. Papagiannakis, Energy harvesting from asphalt pavement roadways vehicle-induced stresses: A feasibility study, Applied Energy, 2016, 182, 210-218.

[19] Y. Zhang, H. Chen, K. Guo, X. Zhang and S.E. Li, Electro-hydraulic damper for energy harvesting suspension: Modeling, prototyping and experimental validation, Applied Energy, 2017, 199, 1-12.

[20] R. Zhang, X. Wang, E.A. Shami, S. John, L. Zuo and C.H. Wang, A novel indirect-drive regenerative shock absorber for energy harvesting and comparison with a conventional direct-drive regenerative shock absorber, Applied Energy, 2018, 229, 111-127.

[21] D. Maurya, P. Kumar, S. Khaleghian, R. Sriramdas, M.G. Kang, R.A. Kishore, V. Kumar, H.-C. Songe, J.-M. Park, S. Taherif and S. Priya, Energy harvesting and strain sensing in smart tire for next generation autonomous vehicles, Applied Energy, 2018, 232, 312-322.

[22] R.K. Sleeper and R.C. Dreher, Tire stiffness and damping determined from static and free-vibration tests, NASA Technical Paper 1671, 1980.

[23] P.A. Misiewicz, T.E. Richards, K. Blackburn and R.J. Godwin, Comparison of methods for estimating the carcass stiffness of agricultural tyres on hard surfaces, Biosystems Engineering, 2016, 147, 183-192.

[24] Z. Liu and Q. Gao, Analytical investigation on tire dynamics by rigid–elastic coupled tire model with nonlinear sidewall stiffness, Journal of the Brazilian Society of Mechanical Sciences and Engineering, 2018, 40(80), 1-14.

[25] Z. Liu, Q. Gao and H. Niu, In-plane flexible beam on elastic foundation with combined sidewall stiffness tire model for heavy-loaded off-road tire, Journal of Dynamic Systems, Measurement, and Control, 2019, 141(6), 061006.

วารสารวิชาการเทคโนโลยีอุตสาหกรรม (The Journal of Industrial Technology)
ISSN (Print): 1686-9869, ISSN (online): 2697-5548
DOI: 10.14416/j.ind.tech.2022.12.001

[26] Y. Xu, M. Freney, R. Hassanli, Y. Zhuge, Md.M. Rahman and Md.R. Karim, Experimental study on the structural performance of full-scale tyre wall for residential housing applications, Engineering Structures, 2022, 259, 114181.

[27] Y. Xu and M. Ahmadian, Improving the capacity of tire normal force via variable stiffness and damping suspension system, Journal of Terramechanics, 2013, 50, 121-132.

[28] A. Soltani, A. Goodarzi, M.H. Shojaeefard and K. Saeedi, Optimizing tire vertical stiffness based on ride, handling, performance, and fuel consumption criteria, Journal of Dynamic Systems, Measurement, and Control, 2015, 137(12), 121004.

[29] Y.F. Lian, Y. Zhao, L.L. Hu and Y.T. Tian, Cornering stiffness and sideslip angle estimation based on simplified lateral dynamic models for four-in-wheel-motor-driven electric vehicles with lateral tire force information, International Journal of Automotive Technology, 2015, 16(4), 669-683.

[30] J. Ni, J. Hu and C. Xiang, Relaxed static stability based on tyre cornering stiffness estimation for all-wheel-drive electric vehicle, Control Engineering Practice, 2017, 64, 102-110.

[31] Y.-W. Kim, Micromechanically consistent calculation of rotational stiffness of radial tire, Journal of Mechanical Science and Technology, 2009, 23, 1294-1305.

[32] Y. Tao, Y. Liu, H. Zhang, C.A. Stevens, E. Bilotti, T. Peijs and J.J.C. Busfielda, Smart cord-rubber composites with integrated sensing capabilities by localised carbon nanotubes using a simple swelling and infusion method, Composites Science and Technology, 2018, 167, 24-31.

[33] J.-J. Bae, Y. You, J.B. Suh and N. Kang, Calculation of the structural stiffeness of run-flat and regular tires by considering strain energy, International Journal of Automotive Technology, 2019, 20(5), 979-987.

[34] J. Li, X. Zhao, Z. Zhang, Y. Xian, Y. Lin, X. Ji, Y. Lu and L. Zhang, Construction of interconnected Al_2O_3 doped rGO network in natural rubber nanocomposites to achieve significant thermal conductivity and mechanical strength enhancement, Composites Science and Technology, 2020, 186, 107930.

[35] M.N. Shenvi, H. Mousavi and C. Sandu, Tread rubber compound effect in winter tires: Benchmarking ATIIM 2.0 with classical models, Journal of Terramechanics, 2022, 101, 43-58.

วารสารวิชาการเทคโนโลยีอุตสาหกรรม (The Journal of Industrial Technology)
ISSN (Print): 1686-9869, ISSN (online): 2697-5548
DOI: 10.14416/j.ind.tech.2022.12.001

[36] P.S. Pillai, Inflation pressure effect on whole tyre hysteresis ratio and radial spring constant, Indian Journal of Engineering and Materials Sciences, 2006, 13, 110-116.

[37] J. Winroth, P.B.U. Andersson and W. Kropp, Importance of tread inertia and damping on the tyre/road contact stiffness, Journal of Sound and Vibration, 2014, 333, 5378-5385.

[38] K.R.S. Wright, T.R. Botha and P.S. Els, Effects of age and wear on the stiffness and friction properties of an SUV tyre, Journal of Terramechanics, 2019, 84, 21-30.

[39] C. Becker and S. Els, Agricultural tyre stiffness change as a function of tyre wear, Journal of Terramechanics, 2022, 102, 1-15.